Zhang, Z., Chen, S.-S., Sun, D.-W., and Gao, S., 2023, Coexisting Nb-enriched basalts and arc volcanic rocks in the northern Qiangtang Terrane, China: Implications for the effects of ambient mantle on subduction zone magmatism: GSA Bulletin, https://doi.org/10.1130/B36847.1.

Supplemental Material

Figure S1. Zircon CL images and labelled the U-Pb dating spots.

Figure S2. Ilmenite transillumination image and labelled the ICP–MS spots.

Table S1. Zircon U-Pb data for the volcanic rocks from the Tuotuohe region of the northern Qiangtang Terrane.

Table S2. Trace element data of the ilmenite in NEBs from the Tuotuohe region of the northern Qiangtang Terrane.

Table S3. Model parameters used in mixing and melting calculations as shown in Figure 10D.

Supplementary Materials

Coexisting Nb-enriched basalts and arc volcanic rocks in the northern Qiangtang Terrane, China: Implications for the effects of ambient mantle on subduction zone magmatism

Ze Zhang[1], Sheng-Sheng Chen[1,2,3 †], Da-Wei Sun[1], and Sen Gao[1]

[1]State Key Laboratory of Geological Processes and Mineral Resources, and School of Earth Science and Resources, China University of Geosciences, Beijing 100083, China
[2]Institute of Tibetan Plateau Research, Chinese Academy of Sciences, Beijing 100101, China;
[3]University of Chinese Academy of Sciences, Beijing 100049, China

Supplementary material contains zircon CL images (Figure S1), ilmenite transillumination image (Figure S2), references for the Permian to Triassic magmatic rocks in the northern Qiangtang in Figures 1A and 3B, analytical results for zircon U–Pb data (Table S1), trace element data of the ilmenite in NEBs (Table S2), and model parameters used in mixing and melting calculations in Figure 10D (Table S3).

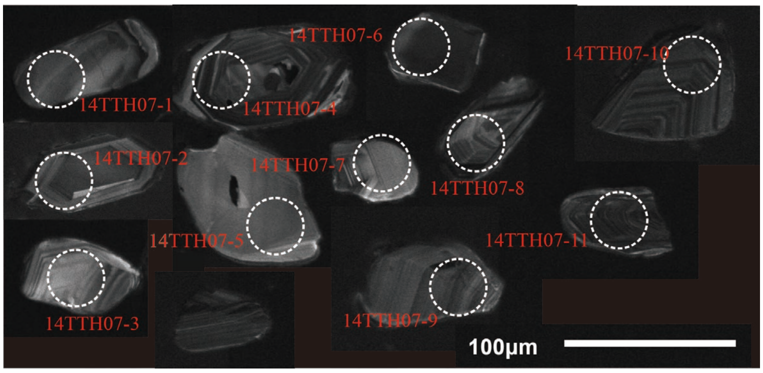

Figure S1. zircon CL images and labelled the U-Pb dating spots

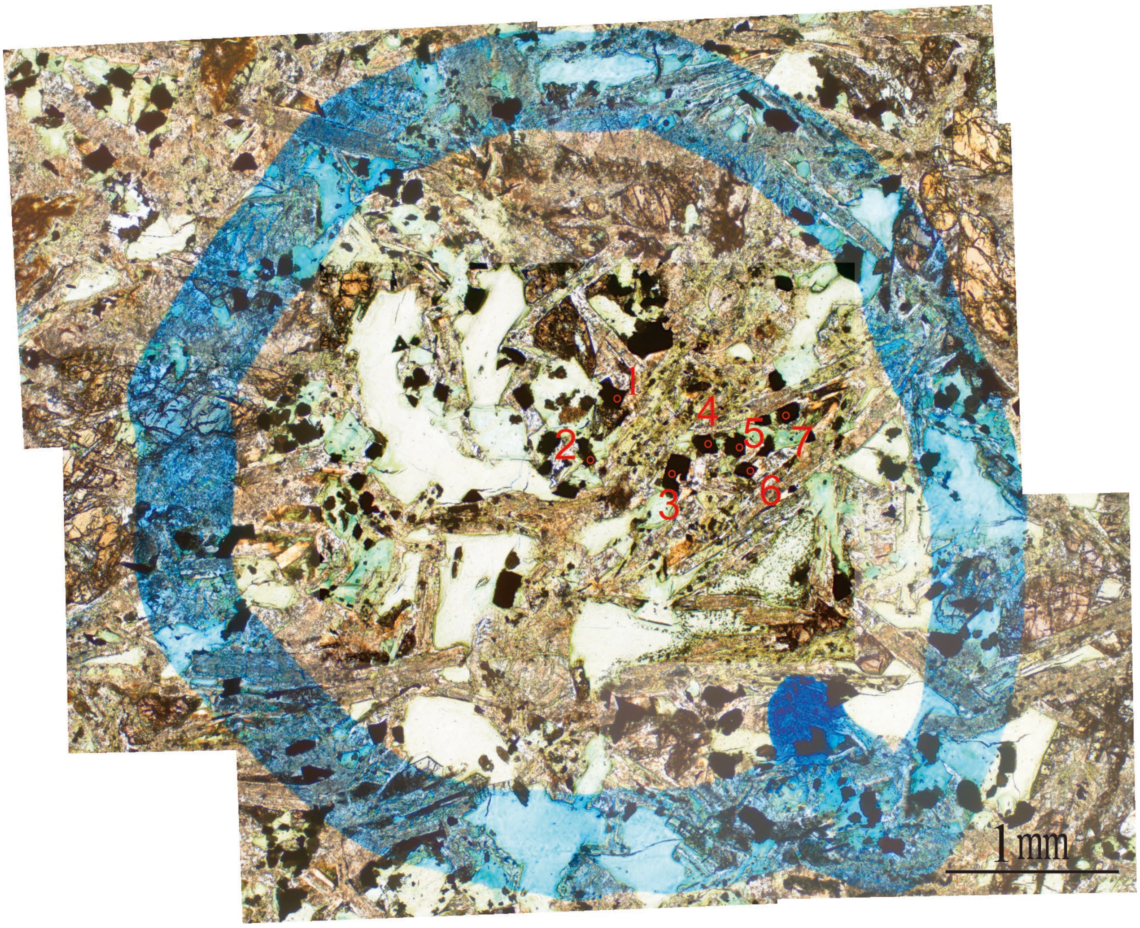

Figure S2. ilmenite transillumination image and labelled the ICP–MS spots

References for the Permian to Triassic magmatic rocks in the northern Qiangtang in Figures 1A and 3B:

Chen, J. W., Li, C., Hu, P. Y., Xie, C. M., Peng, H., & Jiang, Q. Y. (2014). LA-ICP-MS zircon U-Pb age and geochemical characteristics of the granodiorite in the Riwanchaka area, central Qiangtang. Geological Bulletin of China, 33(11), 1750–1758 (in Chinese with English abstract).

Chen, S. S., Shi, R. D., Fan, W. M., Zou, H. B., Liu, D. L., Huang, Q. S., Gong, X. H., Yi, G. D., & Wu, K. (2016a). Middle Triassic ultrapotassic rhyolites from the Tanggula Pass, southern Qiangtang, China: A previously unrecognized stage of silicic magmatism. Lithos, 264, 258–276.

Chen, S. S., Shi, R. D., Yi, G. D., & Zou, H. B. (2016b). Middle Triassic volcanic rocks in the Northern Qiangtang (Central Tibet) :Geochronology, petrogenesis, and tectonic implications. Tectonophysics, 666, 90–102.

Fan, J. J., Li, C., Xie, C. M., Liu, Y. M., Xu, J. X., & Chen, J. W. (2017). Remnants of late Permian–Middle Triassic ocean islands in northern Tibet: Implications for the late-stage evolution of the Paleo-Tethys Ocean. Gondwana Research, 44, 7–21.

Fu, X. G., Wang, J., Wang, Z. J., Chen, W. X. (2008). U-Pb zircon age and geochemical characteristics of volcanic rocks from the Juhua mountain area in the northern Qiangtang basin, northern Xizang (Tibet). Geological Review, 54(2), 232–242 (in Chinese with English abstract).

Fu, X. G., Wang, J., Tan, F. W., Chen, M., & Chen, W. B. (2010a). The Late Triassic rift-related volcanic rocks from eastern Qiangtang, northern Tibet (China): Age and tectonic implications. Gondwana Research, 17, 135–144. https://doi.org/10.1016/j.gr.2009.04.010

Fu, X. G., Wang, J., Chen, W. B., & Feng, X. L. (2010b). Age and tectonic implication of the late Triassic NadiKangri volcanic rocks in the Qiangtang basin, northern Tibet, China. Journal of Chengdu University of Technology (Science and Technology Edition), 37(6), 605–615 (in Chinese with English abstract).

Guan, J. L., Geng, Q. R., Peng, Z. M., Zhang, Z., Wang, G. Z., & Chen, Y. Y. (2016). Petrology, petrochemistry and Zircon U-Pb dating and Hf isotope features of Xiamari granites in Tanggula magmatic belt, Qinghai-Tibet Plateau. Acta Geologica Sinica, 90(2),304–333 (in Chinese with English abstract).

Hu, P. Y., Yang, H. T., Zhang, H. B., & Yu, H. (2010a). Characteristic, zircon dating and tectonic significance of Late Triassic granite in the Guoganjianianshan area, central Qiangtang, Qinghai-Tibet Plateau, China. Geological Bulletin of China, 29(12), 1825–1832 (in Chinese with English abstract).

Hu, P. Y., Li, C., Su, L., Li, C. B., & Yu, H. (2010b). Zircon U-Pb dating of granitic gneiss in Wugong Mountain area, central Qiangtang, Qinghai-Tibet Plateau: age records of Pan-African movement and Indo-China movement. Geology in China, 37(4), 1050–1061 (in Chinese with English abstract).

Hu, P. Y., Li, C., Jie, C. M., Wang, M., Li, J., & Zhong, L. X. (2014). Zircon U-Pb dating and Hf-isotope compositions of granodiorite from the Guoganjianian Mountain area, central Qiangtang, northern Tibet, China. Northwest Geology, 47(1), 52–60 (in Chinese with English abstract).

Hu, P. Y., Li, C., Li, J., Wang, M., Xie, C. M., & Wu, Y. W. (2014). Zircon U–Pb–Hf isotopes and whole-rock geochemistry of gneissic granites from the Jitang complex in Leiwuqi area, eastern Tibet, China: Record of the closure of the Paleo-Tethys Ocean. Tectonophysics, 623, 83–99.

Jin, X., Zhang, Y. X., Zhou, X. Y., Zhang, K. J., Li, Z. W., Khalid, S. B., Hu, J. C., Lu, L., & Sun, W. D. (2019). Protoliths and tectonic implications of the newly discovered Triassic Baqing eclogites, central Tibet: Evidence from geochemistry, Sr-Nd isotopes and geochronology. Gondwana Research, 69, 144–162.

Kapp, P., Yin, A., Manning, C. E., Harrison, T. M., Taylor, M. H., & Ding, L. (2003). Tectonic evolution of the early Mesozoic blueschist-bearing Qiangtang metamorphic belt, central Tibet. Tectonics, 22(4), 1043–1053.

Li, B., Xiang, S. Y., Feng, D. X., Luola, C. W., Gasang, D. Z., & Zhou, Y. (2012). LA-ICP-MS zircon U-Pb age and tectonic setting of Mesozoic granite in Chala area, Caiya Country, eastern Tibet. Geological Bulletin of China, 31(5), 696–706 (in Chinese with English abstract).

Li, C. (1997). The 40Ar/39Ar age and its significance of the crossite from the blueschist in the Mid-Qiangtang area, Tibet. Chinese Science Bulletain, 42(1), 88 (in Chinese with English abstract).

Li, C., Zhai, Q. G., Chen, W., Yu, J. J., Huang, X. P., & Zhang, Y. (2006). Ar-Ar chronometry of the eclogite from central Qiangtang area, Qianghai-Tibet Plateau. Acta Petrologica Sinica, 22(12), 2843–2849 (in Chinese with English abstract).

Li, C., Zhai, Q. G., Chen, W., Yan, Q. R., Dong, Y. S., & Yu, J. J. (2007). Geochronology evidence of the closure of Longmu Co-Shuanghu suture, Qinghai-Tibet plateau: Ar-Ar and zircon SHRIMP geochronology from ophiolite and rhyolite in Guoganjianian. Acta Petrologica Sinica, 23(5), 911–918 (in Chinese with English abstract).

Li, C., Dong, Y. S., Zhai, Q. G., Yu, J. J., & Huang, X. P. (2008). High-pressure metamorphic belt in Qiangtang, Qinghai-Tibet Plateau, and its tectonic significance. Geological Bulletin of China, 27(1), 27–35 (in Chinese with English abstract).

Li, G. M., Li, J. X., Zhao, J. X., Qing, K. Z., Cao, M. J., & Evans, N. J. (2015). Petrogenesis and tectonic setting of Triassic granitoids in the Qiangtang terrane, central Tibet: Evidence from U–Pb ages, petrochemistry and Sr–Nd–Hf isotopes. Journal of Asian Earth Sciences, 105, 443–455.

Li, J. C., Zhao, Z. B., Zheng, Y. L., Yuan, G. L., & Liang, X. (2015). The magmatite evidences in southern Qiangtang for paleo-Tethys ocean subducting collision: Gangtang-co granites in Rongma, Tibet. Acta Petrologica Sinica, 31(7), 2078–2088 (in Chinese with English abstract).

Li, Z. X., Xie, S. K., He, J. L., Xiong, S., Wu, T., & Deng, Q. (2014). LA-ICP-MS U-Pb zircon dating of dioritic gneiss and its geochemical characteristics in the Lianggehu region, Qiangtang Basin. Acta Geologica Sinica, 88(1), 15–24 (in Chinese with English abstract).

Liu, H., Wang, B. D., Ma, L., Cao, R., Li, C., Li, X. B., & Wang, L. Q. (2016). Late Triassic syn-exhumation magmatism in central Qiangtang, Tibet: Evidence from the Sangehu adakitic rocks. Journal of Asian Earth Sciences, 132, 9–24. https://doi.org/10.1016/j.jseaes.2016.10.009

Liu, T., Zhai, Q. G., Wang, J., Su, L., Kang, Z., & Suolang, C. L. (2013). LA-ICP-MS zircon U-Pb age of high-grade metamorphic rocks from the Qiangtang Basin, northern Tibet, and its geological implication. Geological Bulletin of China, 32(11), 1691–1703 (in Chinese with English abstract).

Lu, L., Zhang, K. J., Yan, L. L., Jin, X., & Zhang, Y. X. (2017). Was Late Triassic Tanggula granitoid (central Tibet, western China) a product of melting of underthrust Songpan-Ganzi flysch sediments? Tectonics, 36, 1–27. https://doi.org/10.1002/2016TC004384

Ma, L., Li, Z. X., Li, Y., Liu, H., Wu, C. S., Wei, H. W., & Deng, Q. (2016). Zircon U-Pb age, geochemical characteristics and geological significance of Shanzixingshan basalt in Shuang, Northern Tibet. Geoscience, 30(4), 748–759 (in Chinese with English abstract).

Peng, T. P., Zhao, G. C., Fan, W. M., Peng, B. X., & Mao, Y. S. (2015). Late Triassic granitic magmatism in the Eastern Qiangtang, Eastern Tibetan Plateau: Geochronology, petrogenesis and implications for the tectonic evolution of the Paleo-Tethys. Gondwana Research, 27, 1494–1508. https://doi.org/10.1016/j.gr.2014.01.009

Pullen, A., Kapp, P., Gehrels, G. E., Vervoort, J. D., & Ding, L. (2008). Triassic continental subduction in central Tibet and Mediterranean-style closure of the Paleo-Tethys Ocean. Geology, 36(5), 351–354. https://doi.org/10.1130/G24435A

Qiangba, Z. X., Xie, Y. W., Wu, Y. W., Xie, C. M., Li, Q. L., & Qiu, J. Q. (2009). Zircon SIMS U-Pb dating and its significance of cumulate gabbro from Dengqen ophiolite, eastern Tibet, China. Geological Bulletin of China, 28(9), 1253–1258 (in Chinese with English abstract).

Qiu, J. Q., Qiangba, Z. X., Li, H., & Laba, C. R. (2011). Discovery and characteristic of the Danong slices in the Lancangjiang suture in the middle Permian period. Geological survey and research, 34(4), 258–267 (in Chinese with English abstract).

Shi, C., Li, R. S., He, S. P., Wang, C., Pan, S. J., Zhang, H. D., & Gu, P. Y. (2012). Zircon U-Pb dating, geochemical and geological significances studies for gneissic biotite monzogranite in Riwoqe County, Tibet. Xinjiang Geology, 30(4), 456–464 (in Chinese with English abstract).

Tao, Y., Bi, X. W., Li, C. S., Hu, R. Z., Li, Y. B., & Liao, M. Y. (2014). Geochronology, petrogenesis and tectonic significance of the Jitang granitic pluton in eastern Tibet, SW China. Lithos, 184–187, 314–323. https://doi.org/10.1016/j.lithos.2013.10.031

Wang, B. D., Wang, L. Q., QiangBa, Z. X., Zeng, Q. G., Zhang, W. P., Wang, D. B., & Cheng, W. H. (2011). Early Triassic collision of northern Lancangjiang Suture: Geochronological, geochemical and Hf isotope evidences from the granitic gneiss in Leiwuqi area, East Tibet. Acta Petrologica Sinica, 27(9), 2752–2762 (in Chinese with English abstract).

Wang, G. H., Jia, J. C., Wan, Y. P., Zhang, W. J., Zhou, Z. G., Li, Q. S., & Yang, G. D. (2006). Forming and tectonic significance of the Youxi tectono-schistose formation, north Baqen county, eastern Tibet. Earth Science Frontiers, 13(4), 180–187 (in Chinese with English abstract).

Wang, J., Wang, Z. J., Chen, W. X., Fu, X. G., & Chen, M. (2007). New evidences for the age assignment of the Nadi Kangri formation in the North Qiangtang basin, northern Tibet, China. Geological Bulletin of China, 26(4), 404– 409 (in Chinese with English abstract).

Wang, J., Fu, X. G., Chen, W. X., Tan, F. W., Wang, Z. J., Chen, M., & Zhuo, J. W. (2008). Geochronology and geochemistry of the volcanic rocks in the Aorushan area, northern Qiangtang. Science in China (Series D: Earth sciences), 38(1), 33–43 (in Chinese with English abstract).

Wang, J., Wang, Q., Zhang, C., Dan, W., Qi, Y., Zhang, X. Z., & Xia, X. P. (2018). Late Permian bimodal volcanic rocks in the northern Qiangtang Terrane, central Tibet: Evidence for interaction between the Emeishan plume and the Paleo-Tethyan subduction system. Journal of Geophysical Research: Solid Earth, 123.

Wang, Y. S., Qu, Y. G., Sun, Z. G., Zheng, C. Z., Xie, Y. H., & Lu, Z. L. (2007). Characteristics and tectonic setting of volcanic rocks of the Late Triassic Nongbal Formation at the northern margin of the south Qiangtang block, northern Tibet, China. Geological Bulletin of China, 26(6), 682–691 (in Chinese with English abstract).

Wu, H., Li, C., Chen, J. W., & Xie, C. M. (2015). Late Triassic tectonic framework and evolution of Central Qiangtang, Tibet, SW China. Lithosphere, 8(2), 141–149.

Yang, T. N., Zhang, H. R., Liu, Y. X., Wang, Z. L., Song, Y. C., Yang, Z. S., Tian, S. H., Xie, H. Q., & Hou, K. J. (2011). Permo-Triassic arc magmatism in central Tibet: Evidence from zircon U–Pb geochronology, Hf isotopes, rare earth elements, and bulk geochemistry. Chemical Geology, 284, 270–282. https://doi.org/10.1016/j.chemgeo.2011.03.006

Zeng, Q. G., Wang, B. D., Qiangba, Z. X., Nima, C. R., & Li, H. (2010). Zircon Cameca U-Pb dating of granitoid gneisses in the Leiwuqi area of the eastern Tibet, China and its geological implication. Geological Bulletin of China, 29(8), 1123–1128 (in Chinese with English abstract).

Zhai, Q. G., & Li, C. (2007). Zircon SHRIMP dating of volcanic rock from the Nadigangri formation in Juhuashan , Qiangtang , northern Tibet and its geological significance. Acta Geologica Sinica, 81(6), 795–800 (in Chinese with English abstract).

Zhai, Q. G., Li, C., Wang, J., Chen, W., & Zhang, Y. (2009). Petrology, mineralogy and 40Ar/39Ar chronology for Rongma blueschist from central Qiangtang, northern Tibet. Acta Petrologica Sinica, 25(9), 2281–2288 (in Chinese with English abstract).

Zhai, Q. G., Zhang, R. Y., Jahn, B. M., Li, C., Song, S. G., & Wang, J. (2011). Triassic eclogites from central Qiangtang, northern Tibet, China: Petrology, geochronology and metamorphic P–T path. Lithos, 125, 173–189.

Zhai, Q. G., Jahn, B. M., Su, L., Wang, J., Mo, X. X., Lee, H. Y., Wang, K. L., & Tang, S. H. (2013). Triassic arc magmatism in the Qiangtang area, northern Tibet: Zircon U–Pb ages, geochemical and Sr–Nd–Hf isotopic characteristics, and tectonic implications. Journal of Asian Earth Sciences, 63, 162–178. https://doi.org/10.1016/j.jseaes.2012.08.025

Zhang, H. R., Hou, Z. Q., Yang, T. N., Song, Y. C., Li, Z., Wang, Z. L., Wang, X. H., Wang, Y. K., & Liu, Q. (2010). Subduction-related quartz syenite porphyries in the eastern Qiangtang terrane, Qinghai-Xizang Plateau: Constraints from geochemical analyses. Geological Review, 56(3), 403–412 (in Chinese with English abstract).

Zhang, H. R., Yang, T. N., Hou, Z. Q., Dai, M. N., & Hou, K. J. (2017). Permian back-arc basin basalts in the Yushu area: New constrain on the Paleo-Tethyan evolution of the north-central Tibet. Lithos, 286–287, 216–226.

Zhang, K. J., Tang, X. C., Wang, Y., & Zhang, Y. X. (2011). Geochronology, geochemistry, and Nd isotopes of early Mesozoic bimodal volcanism in northern Tibet, western China: Constraints on the exhumation of the central Qiangtang metamorphic belt. Lithos, 121, 167–175.

Zhang, X. Z., Dong, Y. S., Li, C., Deng, M. R., Zhang, L., & Xu, W. (2014). Tectonic setting and petrogenesis mechanism of late Triassic magmatism in Central Qiangtang, Tibetan Plateau: Take the Xiangtaohu pluton in the Hongjishan region as an example. Acta Petrologica

Sinica, 30(2), 547–564 (in Chinese with English abstract).
Zhang, Y. X., Jin, X., Zhang, K. J., Sun, W. D., Liu, J. M., Zhou, X. Y., & Yan, L. L. (2018). Newly discovered Late Triassic Baqing eclogite in central Tibet indicates an anticlockwise West–East Qiangtang collision. Scientific Reports, 8(966).
Zhu, T. X., Zhang, Q. Y., Feng, X. T., Dong, H., Yu, Y. S., & Li, H. R. (2010). 40Ar/39Ar isotopic dating of the Glaucophane in Caiduo Caka, central Qiangtang area, northern Tibet, China and its geological significance. Acta Geologica Sinica, 84(10), 1448–1456 (in Chinese with English abstract).
Li, H. B., Zhang, Z. C., Santosh, M., Lu, L. S., Han, L., Liu, W., & Cheng, Z. G. (2016). Late Permian basalts in the northwestern margin of the Emeishan large igneous province: Implications for the origin of the Songpan-Ganzi terrane. Lithos, 256, 75–87.
Liu, B., Ma, C. Q., Guo, P., Sun, Y., Gao, K., & Guo, Y. H. (2016). Evaluation of Late Permian mafic magmatism in the central Tibetan Plateau as a response to plume-subduction interaction. Lithos, 264, 1–16.

Table S1

Zircon U-Pb data for the volcanic rocks from the Tuotuohe region of the northern Qiangtang Terrane.

	RATIOS						AGES (Ma)					
Sample	$^{207}Pb/^{206}Pb$	1σ	$^{207}Pb/^{235}U$	1σ	$^{206}Pb/^{238}U$	1σ	$^{207}Pb/^{206}Pb$	1σ	$^{207}Pb/^{235}U$	1σ	$^{206}Pb/^{238}U$	1σ
14TTH07-1	0.05139	0.00345	0.34168	0.02282	0.04823	0.00063	258	129	298	17	304	4
14TTH07-2	0.05447	0.00373	0.36066	0.02454	0.04803	0.00065	391	130	313	18	302	4
14TTH07-3	0.05017	0.00357	0.32376	0.02292	0.04682	0.00061	203	136	285	18	295	4
14TTH07-4	0.0511	0.00487	0.33494	0.03179	0.04755	0.00069	245	188	293	24	299	4
14TTH07-5	0.05388	0.00389	0.35673	0.02562	0.04803	0.00065	366	139	310	19	302	4
14TTH07-6	0.05152	0.00505	0.34444	0.03357	0.0485	0.00072	264	193	301	25	305	4
14TTH07-7	0.05379	0.00351	0.35751	0.02317	0.04822	0.00064	362	123	310	17	304	4
14TTH07-8	0.04988	0.00344	0.3275	0.02245	0.04763	0.00062	189	131	288	17	300	4
14TTH07-9	0.0487	0.00335	0.32206	0.02205	0.04798	0.00062	133	129	283	17	302	4
14TTH07-10	0.05579	0.00353	0.37371	0.02348	0.04859	0.00065	444	117	322	17	306	4
14TTH07-11	~~0.06032~~	~~0.00542~~	~~0.39769~~	~~0.03546~~	~~0.04783~~	~~0.00074~~	~~615~~	~~168~~	~~340~~	~~26~~	~~301~~	~~5~~

- Common lead was corrected by the common lead correction function Andersen (2002).

References

Anderson, T., 2002. Correction of common lead in U–Pb analyses that do not report ^{204}Pb. Chemical Geology 192, 59–79.

Table S2

Trace element data of the ilmenite in NEBs from the Tuotuohe region of the northern Qiangtang Terrane.

	14TTH04-4-1	14TTH04-4-3	14TTH04-4-4	14TTH04-4-5	14TTH04-4-6	14TTH04-4-7
Li	2.32	1.68	1.36	0.50	3.61	3.29
Be	8.91	5.80	5.60	6.05	15.45	10.25
B	135.02	132.35	101.24	106.56	123.80	128.98
Sc	56.91	37.38	32.31	22.55	30.49	16.41
V	2564.25	1958.64	2779.94	2603.69	1735.76	1645.18
Cr	72.54	46.88	389.98	618.88	727.50	179.96
Co	9.21	11.58	11.17	13.27	14.81	13.42
Ni	30.52	37.50	72.75	71.66	38.11	50.48
Cu	1.08	0.30	0.93	1.46	1.01	0.83
Zn	95.99	97.47	102.34	156.23	71.95	97.08
Ga	2.80	4.97	4.05	3.60	4.13	3.58
Rb	0.29	0.40	0.21	0.25	0.22	0.25
Sr	159.68	148.10	124.50	126.67	120.49	141.77
Y	35.72	30.67	23.83	14.94	23.86	18.70
Zr	690.22	533.54	396.61	535.51	377.84	302.89
Nb	99.06	115.80	88.15	89.65	75.30	83.20
Mo	4.41	2.74	1.98	2.86	2.72	1.61
Ag	0.05	0.09	0.00	0.11	0.00	0.00
Cd	0.00	0.23	0.35	0.41	0.00	0.00
Sn	3.21	3.05	2.99	1.62	2.59	1.72
Sb	0.39	0.56	0.49	0.49	0.45	0.54

Cs	0.15	0.03	0.02	0.14	0.11	0.11
Ba	116.09	115.78	95.53	103.65	76.21	119.23
La	13.57	12.08	11.09	15.09	6.51	12.10
Ce	30.78	24.78	24.39	21.94	16.05	19.95
Pr	4.24	3.36	3.29	1.90	2.43	2.28
Nd	18.77	13.82	14.24	8.16	11.36	9.00
Sm	6.37	3.94	3.97	2.10	4.64	3.11
Eu	2.75	2.18	2.13	0.98	1.69	1.23
Gd	6.06	4.96	4.65	2.57	4.70	2.79
Tb	1.37	1.11	1.08	0.56	1.07	0.71
Dy	9.67	7.23	5.97	3.66	6.30	4.53
Ho	1.89	1.41	1.18	0.81	1.10	0.99
Er	5.17	4.41	2.79	2.56	3.26	2.44
Tm	0.81	0.68	0.53	0.32	0.52	0.45
Yb	6.68	5.96	3.45	3.47	3.80	3.13
Lu	0.97	0.80	0.46	0.49	0.53	0.42
Hf	13.28	8.15	6.83	6.51	7.67	6.06
Ta	4.64	4.18	3.21	3.42	3.39	3.95
W	2.69	1.12	0.90	1.58	1.31	0.46
Hg	0.00	0.00	0.00	0.00	0.00	0.00
Tl	0.02	0.02	0.02	0.03	0.00	0.03
Bi	0.01	0.00	0.00	0.00	0.00	0.00
Pb	106.83	86.16	77.26	51.93	66.93	58.34
Th	0.86	1.27	0.56	0.41	1.46	1.27
U	3.41	2.85	1.70	2.54	2.31	2.32

Table S3

Model parameters used in mixing and melting calculations as shown in Figure 10D.

End-member component/partition coefficient		La	Sm	Yb
Sediment				
Initial compositions (GLOSS)[1]		28.8	5.78	2.76
Bulk partition coefficient (sediment/fluid)[2]		1.7	1.61	3.66
Sediment fluid (F=0.02)		17.08	3.62	0.77
Bulk partition coefficient (sediment/melt)[3]		1.34	1.6	1.68
Sediment melt (F=0.05)		21.77	3.68	1.68
Mantle wedge				
upper lavas	Initial mantle wedge[4]	**0.264**	**0.346**	**0.426**
	Starting composition[5]	1.314	0.597	0.36
lower lavas	Depleted mantle (DM)[6]	0.2	0.3	0.4
	Starting composition[7]	3.4655	0.852	0.652

Note:

1. GLOSS = Global Subducted Sediment: the trace element contents are from Plank & Langmuir (1998).
2. Bulk partition coefficients are from the 700°C-2GPa experimental results of Johnson & Plank (1999).
3. Bulk partition coefficients are from the 900°C-2GPa experimental results of Johnson & Plank (1999).
4. The average value of compositions of the initial mantle wedge are from Zhang et al. (2016).
5. The starting composition is composed of average value of compositions of the initial mantle wedge (Zhang et al., 2016) + 4% sediment fluid.
6. The trace element compositions of depleted mantle (DM) are estimated to be somewhat lower than that of Initial mantle wedge.
7. The starting composition is composed of depleted mantle (DM) + 15% sediment melt.

References

Johnson, M. C., & Plank, T. (1999). Dehydration and melting experiments constrain the fate of subducted sediments. *Geochemistry Geophysics Geosystems*, 1, 1007.

Plank, T., & Langmuir, C. H. (1998). The chemical composition of subducting sediment and its consequences for the crust and mantle. *Chemical Geology*, 145(3-4), 325-394.

Zhang, X. Z., Dong, Y. S., Wang, Q., Dan, W., Zhang, C., Deng, M. R., et al. (2016). Carboniferous and Permian evolutionary records for the Paleo-Tethys Ocean constrained by newly discovered Xiangtaohu ophiolites from central Qiangtang, central Tibet. *Tectonics*, 35(7), 1670-1686.